### Optimization of Thermoelectric Cooler (TEC) -Cooled Closed-End Oscillating Heat Pipe Charged with Degassed, Deionized Water

*Leandro T. De Castro*<sup>1</sup>, *Rizalinda L. De Leon*<sup>2</sup>

<sup>1</sup>Assistant Professor 1, Department of Chemical Engineering, University of the Philippines Los Baños, College, Laguna 4031, Philippines (Author for correspondence: ltdecastro1@up.edu.ph)

<sup>2</sup>Associate Professor, Fuels, Energy and Thermal Systems Laboratory, Department of Chemical Engineering, College of Engineering, University of the Philippines Diliman, Quezon City 1001, Philippines

#### **ABSTRACT**

A three level, three factor Box-Behnken design of experiment was conducted to determine the optimum operating condition and the effects of heat load, fill ratio and tilt-angle on the performance of a thermoelectric cooler (TEC)-cooled closed-end oscillating heat pipe charged with degassed, deionized water. The fitted quadratic model for thermal resistance, device temperatures, and DT evaluated at quasi-steady state condition against heat load of 50 watts to 100 watts, fill ratio of 30 % to 70% and tilt-angle of 30° to 90° were all significant (a=0.05). The three main effects were found to be significant in all response models except for the inclination angle having no significant effect on the average condenser temperature. Interaction of heat load and fill ratio has a negative effect on all the response variables while the quadratic effect of fill ratio is high for the average evaporator temperature and DT. Simultaneous numerical optimization of thermal resistance and evaporator temperature with the goal to minimize both evaporator temperature and thermal resistance yielded a minimum thermal resistance from 0.07305 to 0.08439 D°C/Watts and minimum evaporator temperature from 43.4 to 44.2 °C at 58.24 to 60.70 Watts heat load, 37.25 to 38.64% fill ratio, and 90.0° tilt angle. The functional models obtained can be used as basis for comparison with variations of other parameters affecting oscillating heat pipe (OHP) performance.

Keywords: Box-Behnken, Optimization, Oscillating heat pipe (OHP), Pulsating Heat Pipe (PHP), thermoselectric cooler (TEC)

#### INTRODUCTION

Heat pipes in general have been applied in various industries as heat transferring device utilizing the process of evaporation and condensation of a working fluid in a two-phase flow inside a pipe. Some notable applications of heat pipes include cooling of electronic components, thermal control in high temperature environment such as nuclear power source and spacecraft, recovery of heat from high temperature exhaust streams, preservation from thawing of permafrost around pipe supports and energy conservation for residential building thru

waste heat recovery (Zohuri 2011). Of all the industry where heat pipes are utilized, the electronics industry has the major share of the market.

For the last two decades in the field of microelectronics and electronic devices, the use of heat pipes for heat dissipation have gained much attention due to the continuous increase in power requirements coupled with miniaturization which demands for a higher cooling capacity to ensure reliable operating condition. Due to limits in size and cost, the use of other classes of heat pipes like

meandering capillary tube heat pipe commonly called an oscillating heat pipe (OHP) or pulsating heat pipe (PHP) presented by Akachi *et al.* in early 90s has gained much attention.

One primary design consideration for an oscillating heat pipe is the capillary nature of the fluid inside the tube. The unique pulsating/oscillating action inside the pipe makes the difference in operation with the traditional heat pipe. This characteristic to oscillate is dependent not only on the fluid properties but also on the inner diameter of the heat pipe. The Bond number (Bo), which describes the rate of liquid slug gravitational and surface tension forces in a capillary tube, must be less than 2. This sets the maximum tube diameter for the device to operate as OHP. As stated by Cai *et al.*, for a common liquid such as water, the inner diameter should be less than 3mm to guarantee a capillary action. (Cai, Chen, and Asfia 2006)

The self-sustained oscillation/pulsation in an OHP works primarily due to the pressure gradient induced by the alternating temperature experienced by the train of vapor/liquid system inside the capillary tube. The system perturbation due to the presence of meandering turns contributes to this behavior. The axial movement and phase change of vapor plugs and liquid slugs allows for the transfer of heat thru sensible and latent heat respectively. This combinations of system parameters makes the thermo-hydrodynamic properties of the working fluid important for the successful operation of an OHP (Khandekar and Groll 2004).

Oscillating heat pipe due to its unique operation was also applied in other heat transfer applications like wasted heat recovery to reduce energy consumption in a hot air/gas system (Meena and Rittidech 2008; Wannapakhe *et al.*, 2012), heat transfer device in solar water heater to improve efficiency (Arab, Soltanieh, and Shafii 2012), effective heat transfer component for cryogenic application (Liu *et al.* 2015), and thermal spreader to increase thermal conductance to the host substrate (Yang, Khandekar, and Groll 2009).

As compared with a conventional heat pipe (CHP), an OHP also has an evaporator section on one end and a condenser section on the other end with an

optional adiabatic section in between. Operations wise, one clear advantage of an OHP over CHP is the direction of two phase flow where the vapor and liquid phase flow in the same direction as opposed to countercurrent flow in a CHP which requires some wick structure to prevent condenser flooding and evaporator dry out. Also, the fluid inside an OHP is dominated by capillary force whereas CHP works under the influence of gravity.

In understanding the mechanisms of OHP, a test setup of the basic components are usually fabricated with the option of varying parameter conditions. Aside from the meandering pipes, the condenser and evaporator section varies in different experimental studies. The majority of condenser and evaporator section of an OHP test setup are enclosed in a block wherein the cold and hot water streams flow respectively. Water streams to the blocks circulate to and from a water bath maintained at a desired operating temperature (Rittidech 2003). modification on the evaporator section is the use of electric heater instead of water bath (Khandekar and Groll 2004; Kim et al., 2003; Yoon and Oh 2002). One setup uses air stream as cooling system for the condenser section in combination with an electric heater (Cai, Chen, and Asfia 2006; Rahman et al., 2015). A simplified setup to evaluate transient behavior uses a fixed volume of cooling water enclosed in a well-insulated box at the condenser section (Xian et al., 2010).

In small device cooling applications, thermoelectric coolers (TEC) happens to be a common solution since conventional cooling systems are too bulky. A TEC provides reliable cooling without any moving parts. Hence, this type of device finds its application in various fields such as in electronic device cooling application. In the use of OHP as a heat transferring device covering a certain distance from a heat source to a discharge point, the use of TEC provides a convenient alternative solution in cooling the condenser section instead of using a fluid-block assembly. The peltier elements present in it will act as heat pumps to remove the heat from the condenser section. However, TEC still requires good heat dissipation on one side to achieve higher performance and prevent damage on the elements.

Aside from small device applications, TEC shows a promising solution in zero gravity application. The cooling and heating capability without any fluid and pump involve as what the conventional refrigeration provides makes this solution attractive. In a paper by Bruce and Baudouy (2015), they presented the use of passive long cryogenic pulsating heat pipe to cool down a 10 m long and 12.8 m diameter toroid magnet that will be used to protect the human habitat from ionization damages of Galactic Cosmic Rays during long term mission to deep space (Bruce and Baudouy 2015). Hence, a combination of TEC and OHP applied in this field is feasible especially in passively transporting heat from a heat source to another location.

The operational performance of an OHP is affected by many parameters categorized as geometrical, operational, and physical. Geometrical parameters includes the tube inner diameter, cross sectional shape, length of the evaporator and condenser section, overall length of the device and number of turns. Parameters such as inclination angle, and use of check valves falls on the operational aspect of the device. The physical parameters pertains to the properties of the working fluid and its filling ratio with respect to the inside volume. These factors defines the operational boundaries of an OHP. Khnadekar, S. and Groll, M. (Khandekar and Groll 2004) pointed out that the performance of an OHP is strongly dependent on the flow pattern existing inside a tube, hence factors which affect the flow patterns would affect its performance. In the study made by Xian H., et al. (2010), they found that the influence of filling ratio and inclination angle do not follow a regular trend for different working fluids. Due to its nature of operation, there exists an operational limit for every OHP device being used. Yang H., et al. (2008) studied the thermal performance and operational limit of a closed-loop, pulsating heat pipe (CLPHP) as affected by inner diameter, operational orientation and heat load. Changes in performance level could either be an improvement or degradation of the device. Hence for any new devices assembly like an OHP, the determination of its performance at a given working range is important. From a given operating range, an optimum condition defines the current state of a device. A shift from this optimum operating condition implies a change in device operational

characteristic. In this study, the applied heat load, fill ratio, and angle of inclination were considered affecting thermal resistance, device temperatures and temperature difference between evaporator and condenser section.

One way to characterize a device is through the development of a functional model that defines its performance given its operating variables. The functional model can be utilize to determine device operational specification such as valid application range. It can also facilitate in determining the device performance at various operating conditions and can be used in actual device application. Also, in device calibration and performance testing, a change in functional model parameters may imply changes in device physical attributes or changes in material properties like working fluid deterioration.

Conventionally, the performance of an oscillating heat pipes is evaluated using an experimental setup utilizing cold and hot water bath or thru some modifications for its operation. However, a convenient setup utilizing thermo-electric coolers (TEC) for the condenser section has not been explored in the literature. There is no information on the operating range of a TEC-cooled OHP as affected by fill ratio, angle of inclination and heat load.

The study determined the optimum operating condition of a TEC-cooled closed-end OHP charged with degassed, deionized water using the derived response model. Specifically, the study sought to determine the effects of heat load, fill ratio and inclination angle on the thermal performance and operating temperatures, and to establish numerical models relating thermal resistance, operating temperatures and temperature difference between the condenser and evaporator as a function of heat load, fill ratio and inclination angle.

#### **MATERIALS AND METHODS**

#### **Oscillating Heat Pipe Apparatus**

#### Meandering Heat Pipe Assembly

A 14 meandering-turn closed-loop OHP was fabricated by bending a copper tubing (2.0mmID,

3.18mmOD) with a total length of 4.3 meters. The schematic diagram and dimensions used for fabrication are shown in Figure 1. The OHP is equipped with a gate valve (V1) for selection of loop type operation which could either be an open or closed loop. A vacuum valve (V2) serves as opening during vacuum operation of the OHP which is eventually closed when the desired vacuum pressure was achieved. A septum assembly was attached on one of the port for the introduction of fluid into the system using a syringe. Copper tubing connections were soldered and appropriate compression fittings were used for the valves. An Auxiliary piping assembly, equipped with Vacuum gauge (VG60, Supco), was connected to the vacuum valve (V2) to facilitate vacuum operation and flushing.

The OHP can be divided into three main parts: evaporator, adiabatic and condenser section. Both the evaporator and condenser sections of the pipe were enclosed between two 5mm thick stainless sheets 5mm apart with an epoxy potting on the side to contain the thermal grease that fills the inside gap allowing heat conduction from the metal plate to tube outside surface. Thermal grease was introduced into each section using appropriate holes made on one plate that encloses the section and was sealed using a thermal epoxy potting.

#### **Evaporator and Condenser Section**

Heat was supplied to the evaporator plate using a 1-inch wide by 6-feet long (XtremeFlex<sup>TM</sup>) heating tape that was evenly wrapped around the evaporator plate surface. The heater tape was powered using a VARIAC which allows for the variation of supplied current to the heater.

For this assembly, the condenser plate was cooled by four Peltier type thermoelectric cooler (Marlow Industries) linearly distributed across one side of the condenser plate. Each TEC was cooled on one side using an aluminum heat sink with a DC fan powered by a converted 12-volts conventional desktop power supply. Two TEC modules arranged in parallel share one power supply, thus utilizing two DC power supply each having a 2.8 amps setting. The schematic of the evaporator and condenser system is shown in Figure 2. The evaporator and adiabatic sections were insulated with a 5cm thick

Thermawool CT48 Glasswool wrapped with polypropylene tape to fix it from the unit.

#### **Experimental System**

Figure 3 illustrates the experimental setup composed of an OHP assembly that can be tilted and equipped

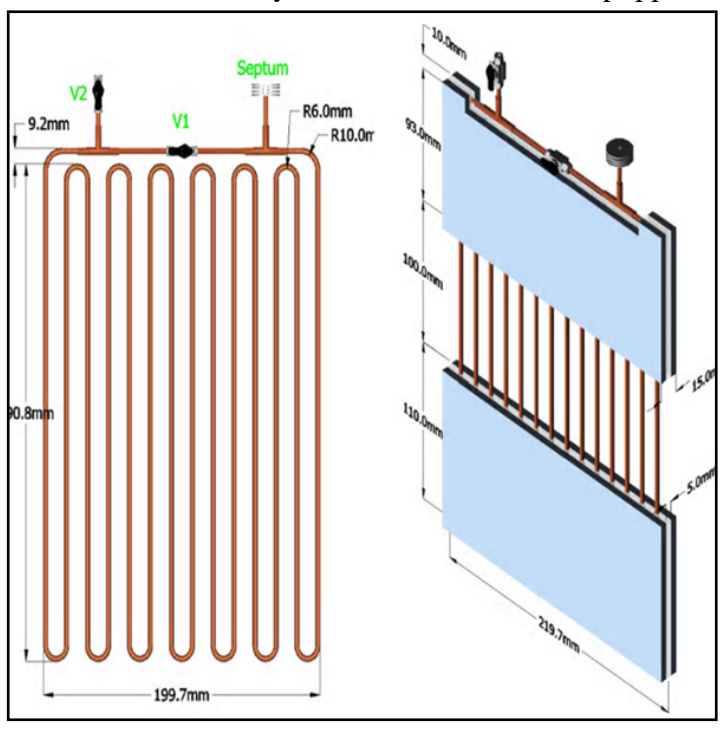


Figure 1. Schematic Diagram of OHP without insulation

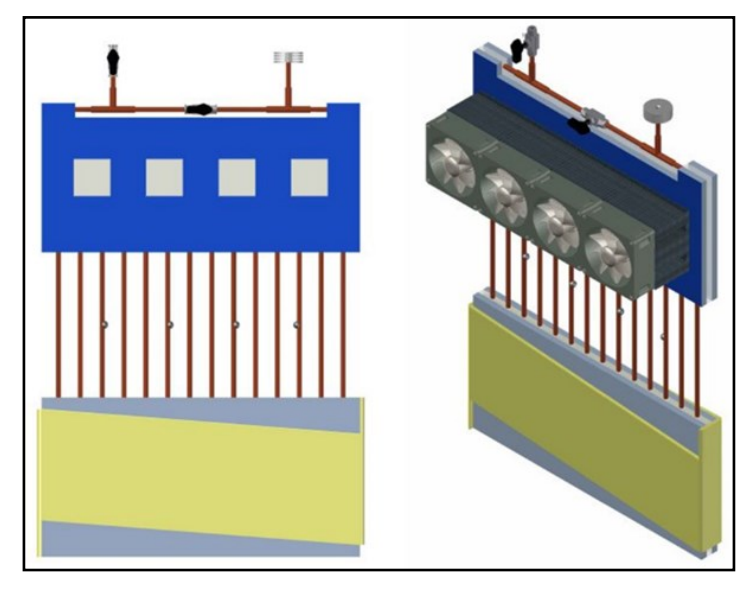


Figure 2. Schematic of Evaporator and Condenser Section

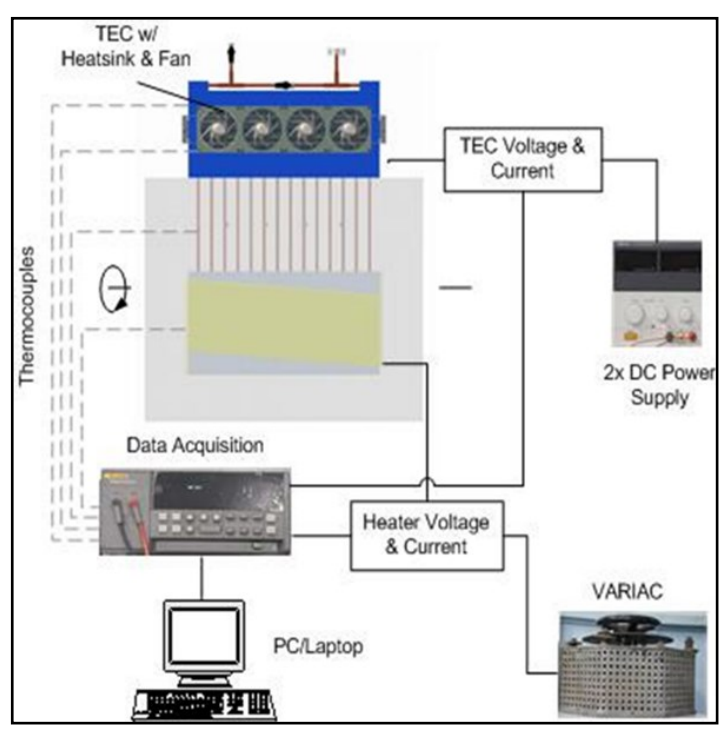


Figure 3. Schematic diagram of experimental set-up

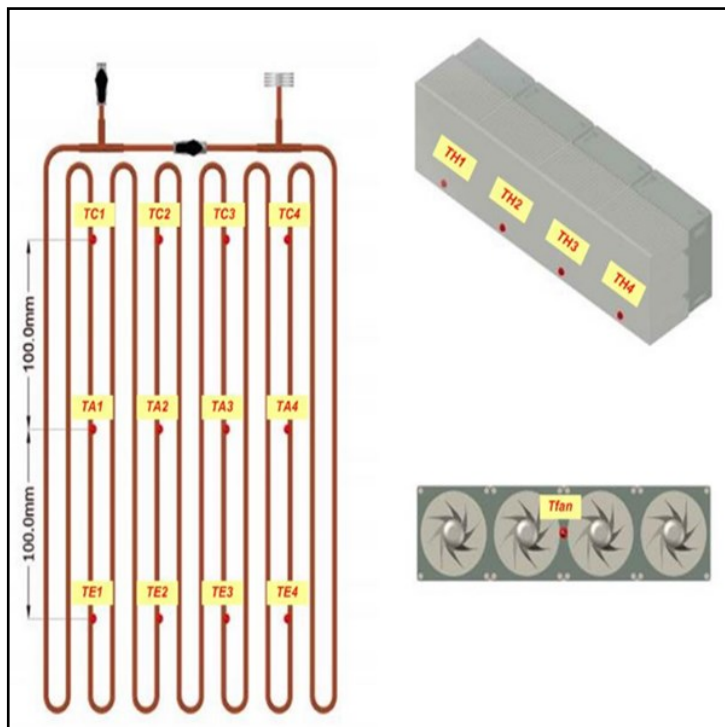


Figure 4. Temperature sensor locations

with a multi-channel data acquisition system (Hydra 2635A), a DC power supply for fan and thermoelectric cooler, and a variable alternating current power supply (VARIAC). thermocouples were situated at each section of the pipe as shown in Figure 4. For the OHP alone, four horizontally-aligned pipe wall temperature for each section were measured. The condenser evaporator thermocouple are located at 100mm distance from the adiabatic thermocouple. The base temperature of the four TEC heat sinks, the inlet fan temperature and ambient room temperature were also measured. Only the pipe wall thermocouple used a K-type while the remaining thermocouples used the T or J type.

#### **Degassing of Deinoized water**

Degassed, deionized (DI) water was prepared using two series of method: boiling and sonication under vacuum. DI water was first boiled in an Erlenmeyer flask with a reflux condenser. After 10 minutes of continuous boiling, the flask was then closed using a rubber stopper and allowed to cool down to room temperature. The liquid was then subjected to sonication under vacuum until the bubble formation, which implies removal of remaining gas dissolved in water, ceased. The degassed deionized liquid was stored into a 10-ml syringe to prevent air contact prior to charging.

#### **OHP Charging and Start-up**

After ensuring that no working fluid was left inside the OHP, that the desired vacuum pressure was achieved and that the OHP is at room temperature, it was then charged with the working fluid at the desired filling ratio via the charging septum using a 10 mL syringe containing the working fluid. Due to the pressure difference brought about by the vacuum inside the OHP, the working fluid was charged to the OHP without the need of pushing the syringe.

With the desired fill ratio and tilt angle, the OHP was started by turning on the data logger to record all measured temperature and voltage. With all the fan and TEC switch at the off position, the power supply for the fan and TEC were turned on. After a few minutes of warming up, the TEC fans were

turned on followed by the TEC with at least one minute interval. For each pair of TEC, the DC power supply was operated at constant current of 2.8 amperes. The condenser temperature was then monitored until a steady state temperature was achieved. After which, the VARIAC knob setting was adjusted to the desired heat load and was turned -on. The OHP was then allowed to reach an oscillating state until it reaches a pseudo steady state temperature condition. The thermocouple signals from evaporator, adiabatic and condenser sections, and the voltage readings were then monitored and recorded on the data acquisition system with at least 10 minutes of acquired data. The heat load and Tilt angle were then adjusted to a desired value until a new pseudo-steady state was achieved and the pseudo steady state oscillation was recorded. All runs were conducted at room temperature of 30°C to 34°C.

#### **Condenser Cooling Performance Test**

Proper operation of the TEC-cooled OHP requires equal performance of the four TEC installed. Hence, the condenser cooling curve was determined using the measured temperature of thermocouple TC1 to TC4. From an initial room temperature, the fans and TEC were turned-on consecutively and the temperature measurements were recorded. The power input to each TEC is calculated using the product of the measured voltage across the TEC and the calculated current passing thru the TEC which was calculated using the test switch that measures the voltage across a resistor (R=0.5 Ohms) in series with the TEC. The current is calculated as the ratio of the measured voltage and the known resistance. Table 1 shows the typical measured voltage and current for each TEC used in the condenser.

#### **Experimental Procedure**

The OHP was first charge with the smallest fill ratio following the charging procedure. The fill-ratio, angle of inclination and heat load were varied according to the Box-Behnken design run. For each run, the equipment was allowed to shift from one pseudo-steady state condition to another while continuously capturing the measured temperature for a given experimental run. A ten-minute captured data at pseudo-steady state was used for the

Table 1. Typical Condenser Thermoelectric Cooler setting

Thermoelectric Coolers	TEC1	TEC2	TEC3	TEC4
Voltage, V	7.05	7.53	7.46	7.08
Current, Amps	0.73	0.732	0.813	0.703

Table 2. Box-Behnken Experimental Design with three factors (Heat Load, Tilt Angle, Fill Ratio)

	Coded	l Factor	s	Actual Factor		
Runs	X1	X2	X3	Heat Load, (W)	Tilt Angle, (Deg.)	Fill Ratio, (%)
1	-1	-1	0	50	30	50
2	1	-1	0	100	30	50
3	-1	1	0	50	90	50
4	1	1	0	100	90	50
5	-1	0	-1	50	60	30
6	1	0	-1	100	60	30
7	-1	0	1	50	60	70
8	1	0	1	100	60	70
9	0	-1	-1	75	30	30
10	0	1	-1	75	90	30
11	0	-1	1	75	30	70
12	0	1	1	75	90	70
C	0	0	0	75	60	50
C	0	0	0	75	60	50
С	0	0	0	75	60	50

computation of operational performance. The TEC voltage and current were measured using the test switch that consecutively records the voltage and current depending on the switch setting. The experimental runs were replicated twice to improve confidence to estimate pure error of generated model and detect an effect.

#### **Box-Behnken Design of Experiment**

The Box-Behnken design of experiment used has three factor with three level and three center point data. Table 2 shows the coded factors and the total run combinations. Regression analysis with the quadratic model of each response variables were performed. Analysis of variance for the independent variables were calculated to determine which parameter significantly affects the desired response. The optimum condition that minimizes the thermal resistance and evaporator temperature was determined using their respective reduced regression model.

# RESULTS AND DISCUSSION

### **TEC** cooling performance

Equivalent cooling performance of the four TEC is necessary to provide an equally distributed cooling across The the condenser section. maximum calculated standard deviation for the four condenser section channels was 0.34 Equation 1 shows the lumped thermal system equation where T(t) is the system's temperature at any time t,

T¥ is the ambient temperature, Ti is the initial system temperature, and  $\tau$ t is the thermal time constant. From the response curve, the thermal time constant for each condenser tube wall was determined by fitting the temperature response data into (equation 1) which assumes that the temperature of the system remains uniform during heat transfer and is only a function of time. A plot of the fitted model and actual response curves are shown in Figure 5. The plot shows a small variation in temperature response among the four sets of TEC assembly. The average response time constant is 4.366 minutes with a standard deviation of 0.012 minutes.

$$-\ln \left[ \frac{T(t) - T_{\infty}}{T_{i} - T_{\infty}} \right] = \frac{t}{\tau_{t}}$$
 Equation 1

#### **Quasi-Steady State Condition**

The performance characteristic of an OHP charged with degassed deionized water was evaluated at the

Table 3. Lumped Thermal Equation Fitted Coefficients

_	CON	DENSER T	UBE WALI	L TEMP			
Parameter	C1	C2	С3	C4			
t <sub>t</sub> , min	4.4475	4.3224	4.2111	4.4858			
T∞, °C	13.78	13.52	14.02	13.89			

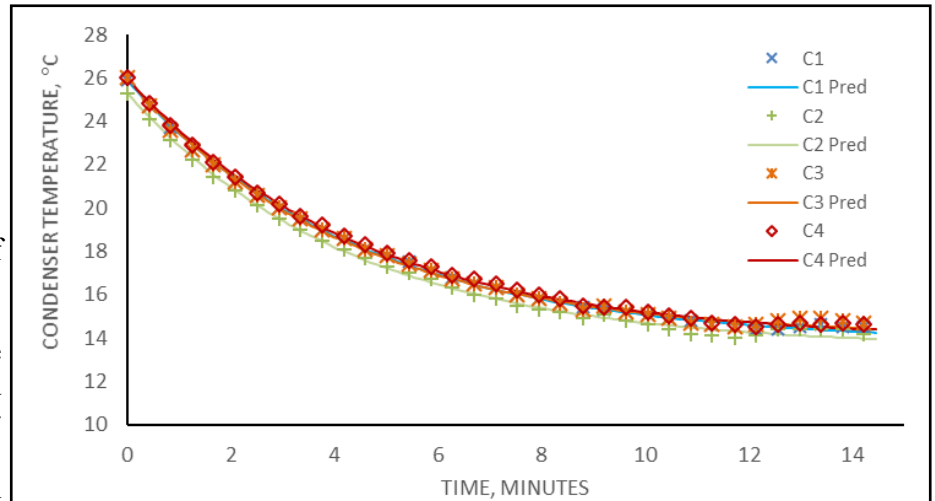


Figure 5. Predicted temperature profile using lumped thermal analysis

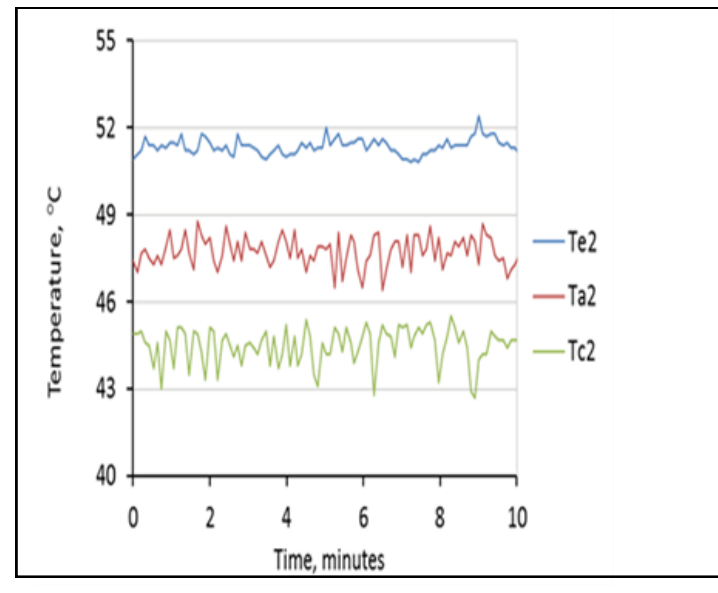


Figure 6. Typical pseudo-steady state OHP wall temperature Profile (75W, 50%FR, 60deg, Ch2)

quasi-steady state condition. Average tube wall temperature at quasi-steady state was calculated from a ten-minute experimental data that has the lowest slope. Figure 6 shows a typical tube wall temperature profile for a single wall Table 4. Model Summary of R-Squared for each Response Variable. temperature at 75 watts heat load, 50% fill ratio and 60 degrees tilt-angle.

## RESPONSE VARIABLE

#### **Quadratic Model Fitting and Analysis of Variance**

Box-Behnken experimental design (BBD) with three factors, three levels was used for the multiple response analysis of a TEC-cooled OHP with five response variables. The fill ratio, tilt-angle and heat load are the numeric factors used in the design Note: \* = suggested, \*\* = aliased while the thermal resistance, evaporator temperature, adiabatic temperature, condenser temperature and DeltaT (Te-Tc) are the desired response variables. Design Expert® (version 7) was used to determine the appropriate model for the given design. Model determination resulted in the use of the suggested quadratic model for all the response variable as shown in table 4. Although the cubic models shows a higher R2, it is aliased and therefore makes the effect of each factor indistinguishable. The fitted model coefficients using regression analysis are given in table 5. Analysis of variance with blocking (for replicates) were performed to

$$\Gamma = \alpha_0 + \alpha_1 H L + \alpha_2 T A + \alpha_3 F R + \alpha_{12} H L \cdot T A + \alpha_{13} H L \cdot F R + \alpha_{23} T A \cdot F R + \alpha_{11} (H L)^2$$
 
$$+ \alpha_{22} (T A)^2 + \alpha_{33} (F R)^2$$
 Equation 2

is given by Equation 2.

determine the significance of the resulting model and model coefficients for each response variable and the results are presented in table 5. The general quadratic model for the response variable

All the quadratic models obtained an acceptable Note: \* = not significant value of coefficient of determination (R<sup>2</sup>) and Adi.  $\mathbb{R}^2$ . This means that the response model obtained for each response variables can explain with 95% confidence the variability in the data. The lack of fit test was significant for DeltaT and thermal resistance model while the evaporator temperature model has relatively low probability (<10%). However, this lack-of-fit test is only one

		RESTOTISE VIRGINEE						
Model	Te, °C	Ta, °C	Tc, °C	Delta T (Te-Tc), °	Thermal Re- sistance, °C/Watts			
	Linear	0.7436	0.8680	0.9869	0.6104	0.6223		
	2FI	0.7762	0.8777	0.9882	0.6589	0.7184		
l	Quad	0.9795 *	0.9836 *	0.9943 *	0.9772 *	0.9645 *		
	Cubic	0.9961 **	0.9957 *	0.9949 **	0.9964 **	0.9974**		

Table 5. Response Model Coefficient in Terms of Coded Factor for the Response Variables

		RESPONSE VARIABLE					
TERMS	Te, °C	Ta, °C	Tc, °C	Delta T, °C	R, °C/W		
Inter- cept	+52.96	+49.53	+46.31	+6.64	+0.087		
A- Heat Load	+8.53	+8.67	+10.74	-2.22	-0.098		
B-Titl Angle	-2.41	-1.60	+3.67E-3*	-2.42	-0.034		
C-Fill Ratio	+7.80	+5.71	-1.31	+9.12	+0.13		
AB	+0.52*	+1.03	-0.070*	+0.59*	+0.020*		
AC	-3.27	-0.83*	+0.17*	-3.44	-0.089		
BC	-1.13*	-0.85*	+0.54*	-1.67	-0.020*		
$A^2$	+2.11	+1.09	-0.048*	+2.15	+0.062		
$\mathbf{B}^2$	+0.70*	+0.58*	-0.31*	+1.00*	+4.82E-4*		
$\mathbb{C}^2$	+8.97	+5.36	-1.23	+10.20	+0.15		

measure of goodness of fit and is affected by the value of pure error where it is compared. In Box-Behnken design, the pure-error is calculated from the values of the center points that are repeated (replicated). Based on the analysis of variance, the sum of squares of pure error is very low as compared with the lack-of-fit sum of squares thereby making the lack of fit test significant. The

Table 6. Quadratic Model Summary Statistics

		Response Variable						
	Te, °C	Ta, °C	Tc, °C	Delta T °C	R, °C/W			
Model	Sig	Sig	Sig	Sig	Sig			
R-Squared	0.9795	0.9836	0.9943	0.9772	0.9645			
Adj R- Squared	0.9698	0.9759	0.9916	0.9664	0.9476			
Pred R- Squared	0.9428	0.9554	0.9865	0.9358	0.8991			
Adeq Precision	30.681	37.520	53.355	27.323	26.017			
Lack of Fit	n.s.	n.s.	n.s.	Sig	Sig			

Table 7. Predicted Range of Response Variable within the Range of Factors

		F	Response	Variable	
Predicted	Te,°C	Ta,°C	Tc, ° C	Delta T (Te-Tc), D°C	Thermal Resistance, D°C/Watts
Maxi- mum	79.5	70.6	57.4	38.3	0.65000
Mini- mum	40.7	39.2	33.0	3.3	0.00674
Range	38.8	31.4	24.4	35.0	0.64326

analysis of variance also suggest that the models can be used to navigate the design space used in the experimental design since the calculated Adeq Precision has a ratio greater than 4 which indicates a good signal-to-noise ratio.

The overall thermal resistance was computed with respect to the device heat load. From the analysis of variance, the quadratic model for the overall thermal resistance is statistically significant at a confidence level of 95%. This demonstrates that the terms in the model have significant effect on the desired response. Analysis of variance shows that all the three main factors are found to be significant including the interaction between heat loads and fill ratio. Among the quadratic terms, only the inclination angle was not significant.

The ANOVA for the evaporator temperature shows that all main factors, the interaction between heat load and fill ratio, and the quadratic term of heat load and fill ratio are significant. Other interaction terms and squared term of the tilt-angle are not

significant. Also the effect of quadratic term of fill ratio on evaporator temperature response is high.

The adiabatic temperature model is significantly affected by the three main effects, interaction term of heat load and tilt-angle, and the squared term of heat load and fill ratio while other model terms are not significant

The condenser section is made of the TEC assembly which is the unique feature of this OHP. From the analysis of variance of the quadratic model, the heat load, fill ratio and the squared term of fill ratio are significant at 95% confidence level while the rest of the terms are not significant.

The temperature difference across the OHP is significantly affected by all model terms except for interacting term of hea load and tilt-angle and the quadratic term of the tilt-angle. The quadratic effect of the fill ratio is also high.

The predicted operating range for the device using the reduced fitted model is given in table 7. The thermal resistance of the device can change from 0.0067 to 0.6500 °C/Watts or a change of around 95 times the lowest predicted thermal resistance. In actual operation, the fill ratio is already set and only the heat load and tilt-angle can change. The highest thermal resistance was predicted at the highest fill ratio of 70%. At this fill ratio, the thermal resistance can change from 0.2080 to 0.6500 °C/Watts or a change of 213%. The increase in fill ratio from 30% to 70% increased the temperature difference (Te-Tc) which suggest a high thermal resistance across the OHP.

#### **Response Surface Analysis**

The regression models obtained for each response variable are used to explain the resulting behavior and performance of the TEC-cooled OHP. Evaluation of the effects of each factor was made with the other factors at the center point.

### Effect of Heat Load

The heat load was found to be significant in all the response models generated. For this TEC-cooled OHP being studied, the tube wall temperature

increases linearly with the increase in heat load. However, the average temperature difference between the evaporator and condenser is negatively affected by the heat load or it decreases as the heat load increases but has a minimal effect. A heated object will initially increase its temperature and eventually reach an equilibrium condition wherein for a given steady-state flow of heat a constant operating temperature profile across the object is maintained. For the case of OHP, the adiabatic temperature may describe the operating temperature. It is evident that the OHP is operating at different adiabatic temperature with the changes in the applied the heat load.

The thermal resistance model obtained from the experimental run shows a decreasing trend with increasing applied heat load. From the study by Ma H., et al. (2006), the effective thermal resistance of an OHP decreases as the operating temperature was increased. Hence the heat transport capability is high at higher operating temperature which is consistent with the decrease in thermal resistance observed at higher heat load as shown in Figure 7.

The low thermal resistance at high heat load that also resulted to high evaporator temperature is also explained by the oscillation characteristic of the fluid. From Figure 8, the range of tube wall adiabatic temperature at 100 watts heat load is smaller compared with that at 50 watts heat load.

The range of adiabatic wall temperature is dependent on the liquid slug flowing at this section of the pipe during oscillation. In the investigation of Zhang and Faghri (2002), found out that they the amplitude of oscillation decreases when the wall temperature of the evaporator section is decreased but the frequency of oscillation is not changed Hence, the increase in evaporator temperature with the increase in heat load would produce a higher amplitude of oscillation of liquid slug in the adiabatic section thereby

reducing the range of local temperature change. The longer a liquid slug will stay in a certain part of the adiabatic section, the longer will be the contact time and would change the wall temperature in a greater degree. As seen in Figure 8, the increase in heat load resulted in the increase of evaporator temperature which resulted in a smaller range in adiabatic tube wall temperature.

Also, regardless of the heat load applied, the temperature range at the condenser section is relatively higher than that of the evaporator section. This same behavior was also shown in the experimental results of Jiao A., *et al.* (2009).

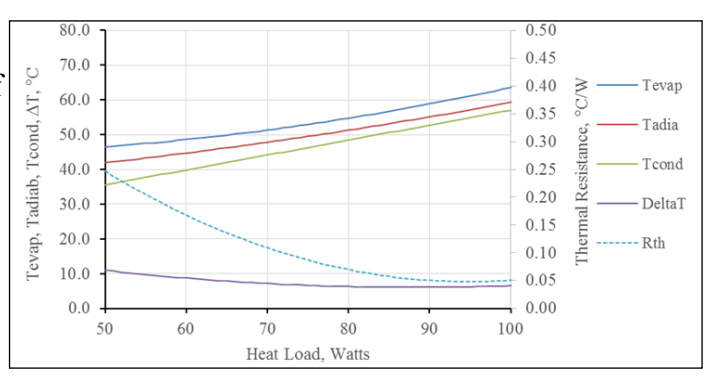


Figure 7. Effect of heat load on quasi-steady state average values of Tevap, Tadia, Tcond, DT and Thermal Resistance (50% FR, 60° TA)

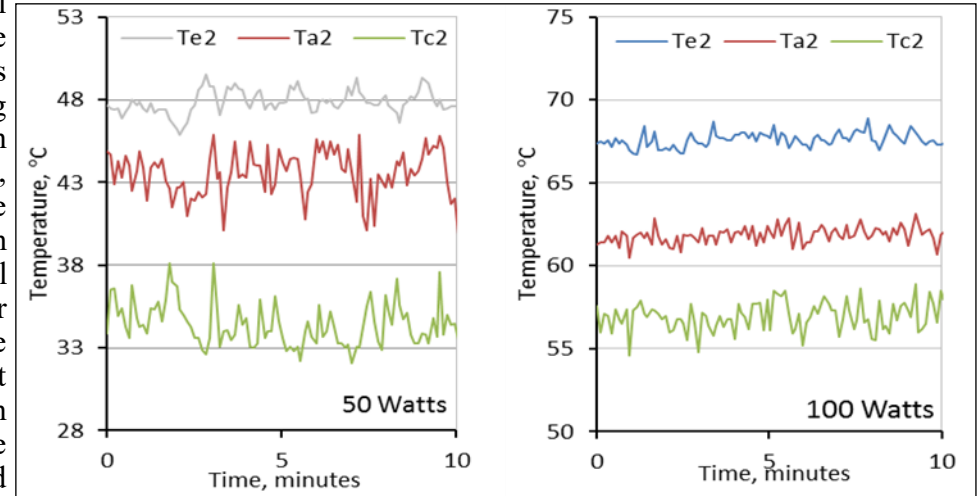


Figure 8. Quasi-steady state Temperature Profile using 50 watts and 100 watts Heat load (50%FR, 30° TA).

The significant effect of the heat load quadratic term (A2) in the response model for thermal resistance suggest a minimum thermal resistance at a certain heat load. An upward trend in thermal resistance is predicted by the model as the heat load is extended beyond 100 Watts. The same phenomena is observed in any heat pipe due to the occurrence of evaporator section drying.

#### Effect of Fill Ratio

The amount of fluid inside an OHP dictates the amount of energy that it can store. The higher the mass of a substance, a much higher amount of energy is needed to achieve the same change in temperature. Since the operating temperature affects the performance of an OHP, it follows that the fill ratio also affects its performance.

As shown in Figure 9, the thermal resistance and the average temperature difference between the evaporator and the condenser have a minimum which can be explained by the strong positive significant effect of its quadratic term. The thermal resistance dramatically increases from the minimal value upon increasing the fill ratio which lowers the heat transport ability of the device.

A small deviation in condenser wall temperature is observed within the range of fill ratio being studied. In the study of Yoon, S. and Oh, C. (2002), they found that at a higher fill charge ratio the working limit of an OHP can be easily reached even at a lower heat load. The increase in calculated thermal resistance is due to the increase in the condenser side thermal resistance since the average temperature difference between the condenser and adiabatic wall is greater than the temperature difference between the evaporator and adiabatic wall. The increase in evaporator temperature is accompanied by increase in adiabatic an temperature and an almost constant condenser wall temperature which implies that the movement of the working fluid is reduced. The minimal movement, hence low amplitude, can be attributed to the increase in internal pressure inside the pipe at higher fill ratio due to lack of vapor space. Also from Figure 10, the range of adiabatic temperature is high at high fill ratio for the same heat load and angle of

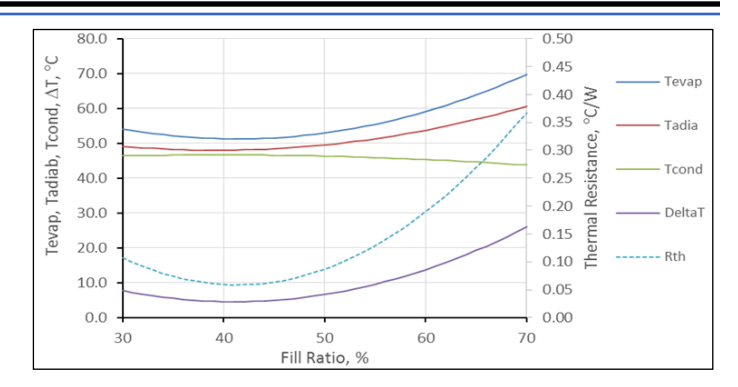


Figure 9. Effect of Fill Ratio on Quasi-steady state values of Tevap, Tadia, Tcond, DT and Thermal Resistance (75W HL, 60° TA)

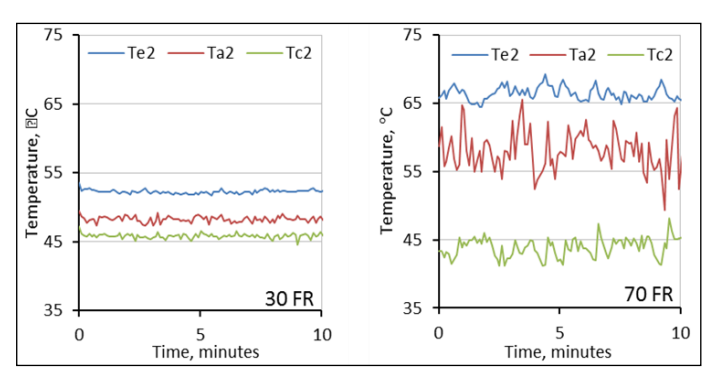


Figure 10. Quasi-steady state Temperature Profile using 30 and 70 Fill Ratio (75W HL, 90° TA)

inclination. This implies a low amplitude of liquid slug oscillating in the adiabatic tube section thereby decreasing the heat transfer thru sensible heat.

#### Effect of Tilt Angle

The effect of gravity on the performance of an OHP is assumed to be negligible due to the dominating capillary forces present inside the pipe. However, in this study, the tilt-angle has a significant effect on all the response variable except on the condenser temperature. In a study by Xian, H. et al. (2014), they observed nonoperation of OHP when operated at limiting condition of horizontal heating. Such stopping of oscillation did not occur for the entire range of factors used in the experiment.

The operation of an oscillating heat pipe depends on fluid internal flow pattern dominating inside the pipe as described by Khandekar, S. and Charoensawan, P. (2009). In their trend analysis, at

an inclination angle greater than 30 degrees, slug and semi-annular flow exist at low heat throughput. At higher heat load, annular flow condition predominantly exists which gives the best thermal performance. However for this study, full annular flow condition is not possible since the OHP is operated as closed-end PHP. Hence internal flow pattern is mostly dominated by slug to semi-annular flow with semi-annular flow pattern dominating at higher inclination angle.

The linear gradual change in the average temperature difference between the evaporator and the condenser as the tilt-angle was increased from 30 to 90 degrees implies no dramatic changes in the flow pattern characteristics (Figure 11). Only a slight decrease in the adiabatic temperature profile range can be observed as shown in Figure 12 for both high and low heat load. For the same amount of heat load, the condenser is operating at almost the same temperature, but the improvement on thermal resistance reduces the evaporator temperature.

#### Significant Interaction Effects

Among the fitted response variables, only the adiabatic temperature response model shows a significant interaction between heat load and tilt-angle (p-value=0.0403). Figure 13 shows the slight positive effect of the interaction for a 30%, 50% and 70% fill ratio. At higher fill ratio, the response plot shifts upward but the slope of the surface remains the same.

The negative interaction between fill ratio and heat load for the average evaporator temperature, Delta T, and thermal resistance is shown in Figure 14. High heat load and fill ratio will reduce the response variable. The worst thermal resistance is at high fill ratio and low heat load while the highest evaporator temperature occurs at high heat load and high fill ratio. Negative interaction effects of heat load and fill ratio on the evaporator temperature response does not translate into a decrease in evaporator temperature due to high individual main effect and positive quadratic effects.

The interaction effect between heat load and fill ratio on thermal resistance is shown Figure 14. At high fill ratio, the thermal resistance decreases with

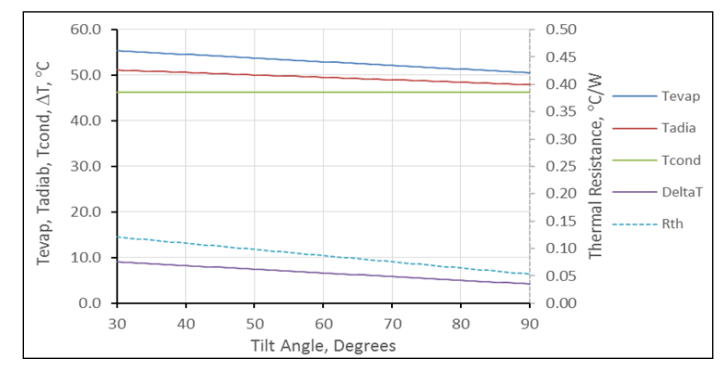
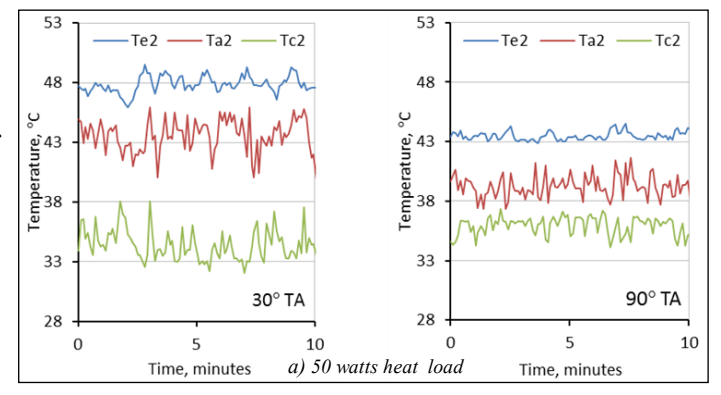


Figure 11. Effect of Tilt Angle on Quasi-steady state values of Tevap, Tadia, Tcond, DT and Thermal Resistance (75W HL, 50% FR)



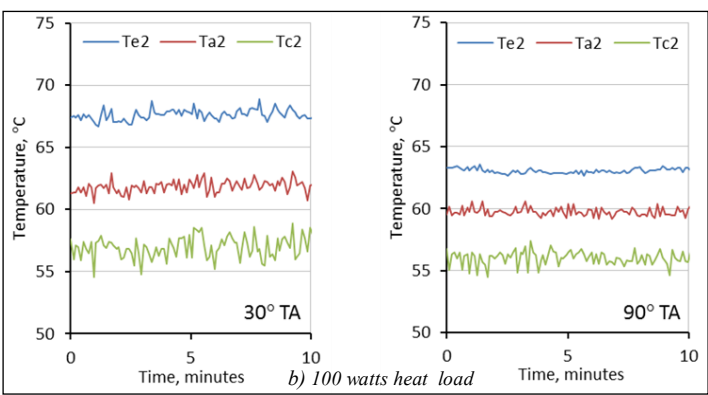


Figure 12. Quasi-steady state temperature profile using 30 and 90 tilt angle (50W&100W HL, 50% FR)

increasing heat load. At a fill ratio of 50%, the plot shifted to a lower value and the slope slightly decreased. A further decrease in fill ratio, the thermal resistance shifted favoring an increasing thermal resistance at higher heat load. This increase in thermal resistance at low fill ratio and high heat load is due to high evaporator temperature. Lesser fluid inside the OHP means lesser fluid returning from the condenser to the evaporator at high heat

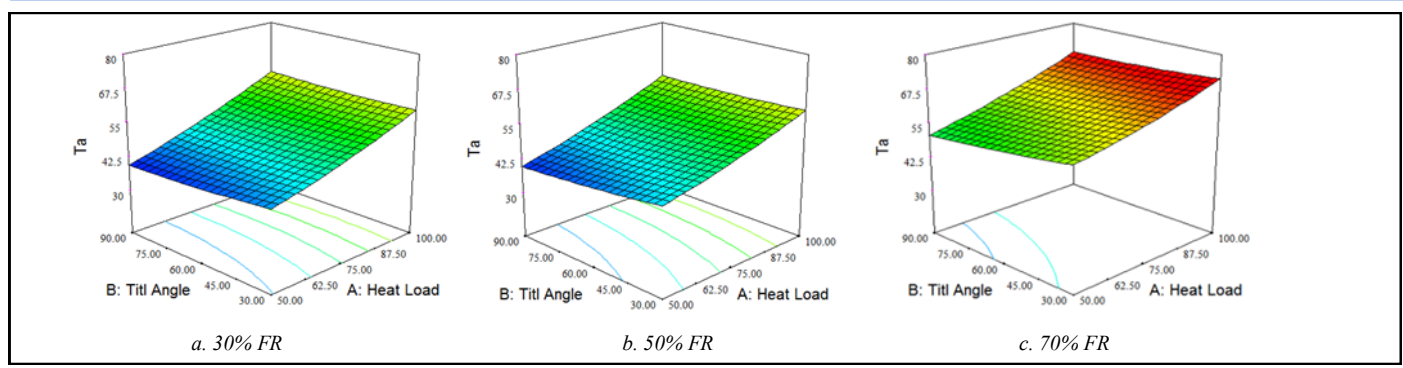


Figure 13. Average adiabatic temperature surface plot for heat load and tilt angle interaction (30% FR, 50% FR, 70% FR)

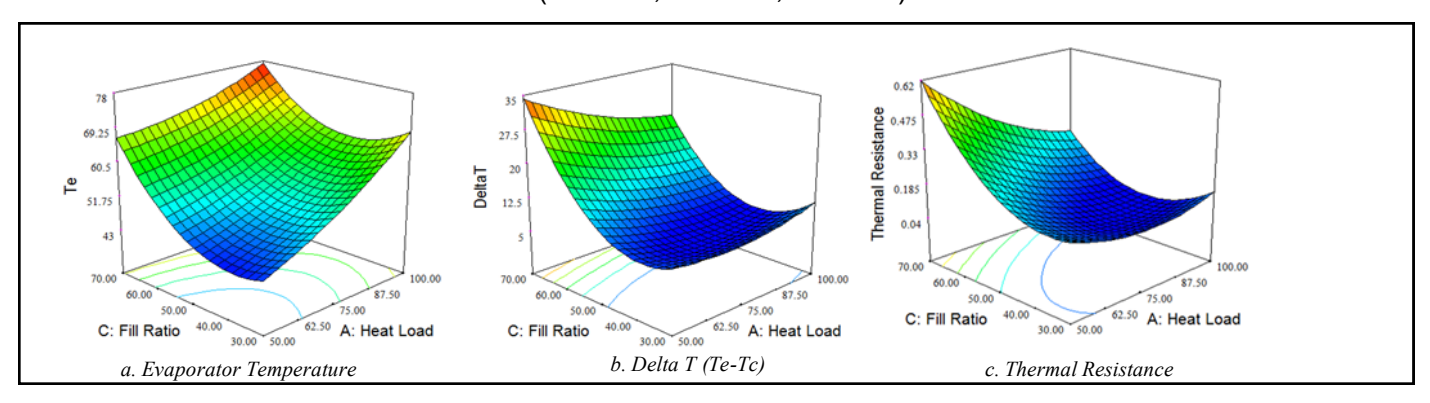


Figure 14. Average Evaporator Temperature (a), Delta T (b), and Thermal Resistance Surface Plot (c) for fill Ratio and heat load interaction (60° TA)

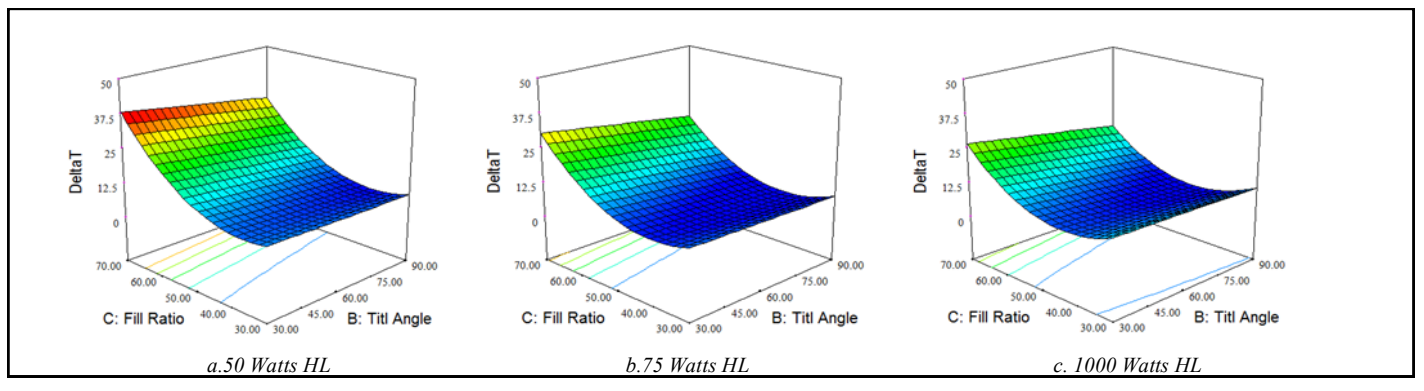


Figure 15. Delta T Surface Plot for Tilt Angle and Fill Ratio Interaction (50W, 75W, 100W HL)

load. With this, the evaporator temperature will increase and will lower the heat transfer performance.

The interaction between fill ratio and tilt angle is only significant in the average difference of evaporator and condenser temperature. A high deltaT happens at high fill ratio and low tilt-angle (Figure 15).

The negative interaction and high quadratic effect of fill ratio contributed to this result.

## Optimization of factors for minimum thermal resistance and evaporator temperature

It can be seen from Figure 14 that the desired low thermal resistance does not coincide with low evaporator temperature. At minimum thermal resistance, the temperature difference between the evaporator and condenser section will be minimal which provides lower evaporator temperature. Using the fitted quadratic model for thermal resistance (Equation 3) in the numerical ptimization tool of Design Expert®, the optimum minimal resistance of 0.00640 D°C/Watts was at thermal heat load of 90.01 watts, 90 degrees tilt angle and 44.6 fill ratio. Table 8 shows several converging solution for thermal resistance optimization. Vertical operation of the OHP provides the lowest thermal resistance. Figure 16 shows the minimum thermal resistance at 90 degrees tilt angle. At the optimum fill ratio, the thermal resistance decreases at the heat load increases up to the optimum heat load. Beyond the optimum heat load, the thermal resistance increases.

Optimum evaporator temperature was also obtained using design expert® with the fitted quadratic model for the three factors. Figure 17 shows the minimum evaporator temperature of 41.06 °C at 50 Watts heat load, 90 degrees tilt angle and 37.63 fill ratio.

$$R_{th} = 0.087 - 0.098 \ HL - 0.034 \ TA + 0.13 \ FR - 0.089 \ HL \cdot FR + +0.062 \ (HL)^2 + 0.15 \ (FR)^2$$
Equation 3

$$T_e = +53.39 + 8.53 \cdot HL - 2.41 \cdot TA + 7.80 \cdot FR - 3.27 \cdot HL \cdot FR + 2.05(HL)^2 + 8.92(FR)^2$$
  
Equation 4

Using design expert® the desirable condition having the same weight level for minimum thermal resistance and minimum evaporator temperature was obtained at several parameter values as shown in Table 10. Having the same desirability value of 0.720, the range of heat load is from 58.24 to 60.70, the range of fill ratio is from 37.25 to 38.64, and the tilt-angle is at 90 degrees. These ranges are different from the optimum conditions obtained when individual response was considered. It can be observed that vertical orientation of the OHP gives the best performance both in thermal resistance and evaporator temperature.

#### CONCLUSIONS

A three level, three factor Box-Behnken design of experiment was used to evaluate the effects of heat load, fill ratio and inclination angle on the

Table 8. Minimum Thermal Resistance Results using Design Expert® Optimization Tool

Number	Heat	Titl	Fill	Thermal
Nullibei	Load	Angle	Ratio	Resistance
1	90.01	90.00	44.60	0.00639
2	91.50	90.00	44.53	0.00664
3	88.30	90.00	43.90	0.00665
4	91.22	90.00	43.62	0.00712
5	83.95	90.00	42.82	0.00924
6	81.58	90.00	42.53	0.01185

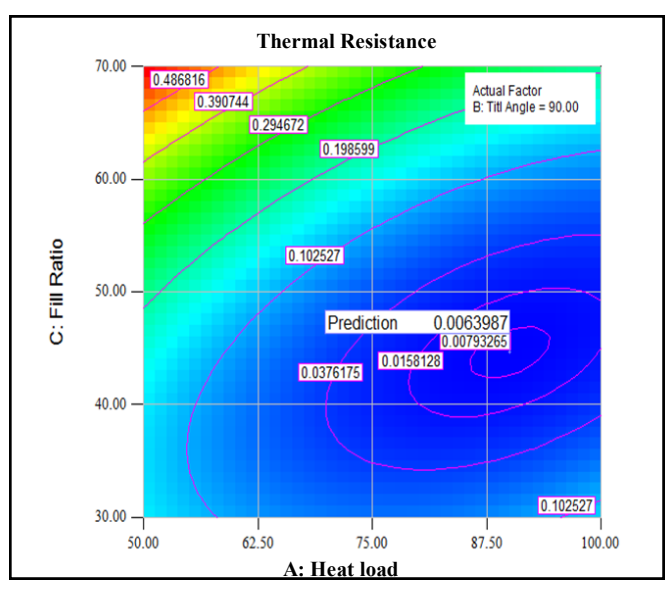


Figure 16. Contour plot of thermal resistance showing optimum parameter values (Tilt Angle, 90°)

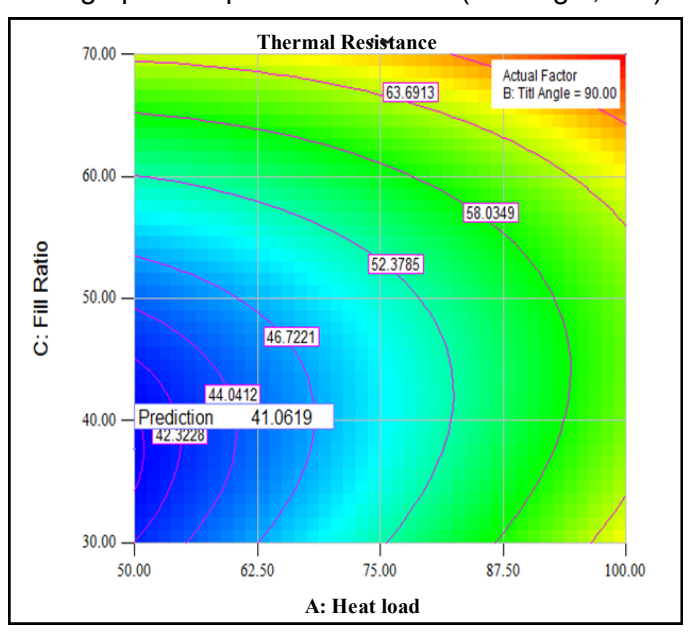


Figure 17. Contour plot of Evaporator Temperature showing optimum parameter values (Tilt Angle, 90°)

performance and to determine the optimum condition of a TEC-cooled OHP charged with degassed, deionized water. Thermal resistance, average temperatures and deltaT were calculated from the quasi-steady state operation of the device. Statistical analysis of the fitted experimental results on a quadratic model, which was the suggested model based on R-square, were made.

It can be said that the condenser temperature of the TEC-cooled OHP is only affected by the main effects of heat load and fill ratio and not by inclination angle and interactions. The interaction of heat load and fill ratio has a negative effect on all response variable. The resulting regression models for the thermal resistance, average temperatures and average temperature difference between evaporator and condenser provides a good fit from the range of effects studied and can be used to navigate the response model to determine the effects of heat load, fill ratio and inclination angle on the performance of an OHP and to determine the operating range of the device. The optimum operating conditions were also determined using the fitted quadratic models for thermal resistance and evaporator temperature. A desirability function was used to determine the optimum operating condition that would give a minimum thermal resistance and minimum evaporator temperature simultaneously. The optimum conditions with a desirability value of 0.72 obtained a range of heat load from 58.24 to 60.70, a range of fill ratio from 37.25 to 38.64 and a tilt-angle of 90 degrees having a minimum thermal resistance from 0.07305 to 0.08439 D°C/Watts and minimum evaporator temperature from 43.4 to 44.2° C.

The experimental results presented in this study can be compared with other OHP experimental data with consideration that the operating temperature of the device is changing as the heat load were change. The functional models developed to determine the optimum operating conditions may be used as basis for comparison with other oscillating heat pipe with design variations and operating range.

#### RECOMMENDATIONS

Instead of using a liquid cooling block assembly at the condenser section which requires a pumping

Table 9. Minimum Evaporator Temperature Results using Design Expert® Optimization Tool

Number	Heat	Tilt	Fill	Te	
	Load	Angle	Ratio		
1	50.00	90.00	37.63	41.1	
2	50.00	89.76	37.94	41.1	
3	50.00	90.00	36.10	41.1	
4	50.00	90.00	39.23	41.1	
5	50.81	90.00	37.39	41.3	
6	50.00	89.99	40.82	41.3	

Table 10. Desirable Condition Results for Minimum Evaporator Temperature and Thermal Resistance using Design Expert® Optimization Tool

DCS.	Design Experts Optimization 1001							
No	Heat	Tilt	Fill	Ther-	Te	Desira-		
	Load	An-	Ratio	mal		bility		
		gle		Re-				
		_		sistance				
1	58.38	90.00	37.87	0.08384	43.4	0.720		
2	58.24	90.00	37.67	0.08439	43.4	0.720		
3	58.71	90.00	37.25	0.08189	43.6	0.720		
4	60.22	90.00	38.64	0.07539	44.0	0.720		
5	60.70	90.00	38.58	0.07305	44.2	0.720		

mechanism, it can be said that TEC may be used as a convenient device to dissipate the heat at the condenser section

The response models obtained can be used as a basis of comparison for future studies related to this TEC-cooled OHP operations. Effects of variations in other parameters to improve OHP performance like changes in the working fluid can be compared for significance using the same experimental method and using the resulting functional models as basis. Also, operation of the device beyond the ranges used in this study can also be evaluated such as horizontal (0 degree) and above heating (-90 degrees).

Additional thermoelectric cooler can be installed on the other side of the condenser plate to enhance the cooling capacity at the condenser section. The operating temperature and applied heat load can then be extended up to the dry out condition to determine the operational limit of the device. Also, additional insulation should be included on the condenser section to reduce heat loss.

To provide the maximum voltage to the TEC, the power supply used for the fans, which is a converted desktop ATX 12 volts power supply, can also be used for the thermoelectric coolers instead of sharing one power supply for two TEC cooler module, which reduces the applied current per module. However, utilizing the TEC at its maximum capacity would also require a high cooling capacity of heat sink and fan assembly for safe operation of the device.

#### **REFERENCES**

- ARAB, M., M. SOLTANIEH, and M.B. SHAFII. (2012). "Experimental Investigation of Extra-Long Pulsating Heat Pipe Application in Solar Water Heaters." Experimental Thermal and Fluid Science 42: 6–15. http://linkinghub.elsevier.com/retrieve/pii/S0894177712000738 (July 10, 2014).
- BRUCE, ROMAIN, and BERTRAND BAUDOUY. (2015). "Cryogenic Design of a Large Superconducting Magnet for Astro-Particle Shielding on Deep Space Travel Missions." Physics Procedia 67: 264–69.
- CAI, QINGJUN, CHUNG-LUNG CHEN, and JULIE F. ASFIA. (2006). "Operating Characteristic Investigations in Pulsating Heat Pipe." Journal of Heat Transfer 128 (12): 1329. http://link.aip.org/link/JHTRAO/v128/i12/p1329/s1&Agg=doi (March 2, 2012).
- JIAO, A J, H B MA, and J K CRITSER. (2009). "International Journal of Heat and Mass Transfer Experimental Investigation of Cryogenic Oscillating Heat Pipes." International Journal of Heat and Mass Transfer 52(15–16): 3504–9. http://dx.doi.org/10.1016/j.ijheatmasstransfer.2009.03.013.
- KHANDEKAR, SAMEER, and PIYANUN CHAROENSAWAN. (2009). "Closed Loop Pulsating Heat Pipes Part A: Parametric Experimental Investigations." Applied Thermal Engineering 23(2003): 2009–20.
- KHANDEKAR, SAMEER and MANFRED GROLL. (2004). "An Insight into Thermo-Hydrodynamic Coupling in Closed Loop Pulsating Heat Pipes." 43: 13–20.
- KIM, JONG-SOO, NGOC HUNG BUI, HYUN-SEOK JUNG, and WOOK-HYUN LEE. (2003). "The Study on Pressure Oscillation and Heat Transfer Characteristics of Oscillating Capillary Tube Heat Pipe." Energy 17(10).
- LIU, YUMENG, HAOREN DENG, JOHN PFOTEN-HAUER, and ZHIHUA GAN. (2015). "Design of a Hydrogen Pulsating Heat Pipe." Physics Procedia 67: 551–56. http://dx.doi.org/10.1016/j.phpro.2015.06.074.

- MA, H. B. *et al.* (2006). "Effect of Nanofluid on the Heat Transport Capability in an Oscillating Heat Pipe." Applied Physics Letters 88(14): 143116. http://link.aip.org/link/APPLAB/v88/i14/p143116/s1&Agg=doi (March 2, 2012).
- MEENA, P, and S RITTIDECH. (2008). "Waste Heat Recovery by Closed-Loop Oscillating Heat Pipe with Check Valve from Pottery Kilns for Energy Thrift." Applied Sciences 1(2): 126–30.
- RAHMAN, M. LUTFOR *et al.* (2015). "An Experimental Investigation on the Effect of Fin in the Performance of Closed Loop Pulsating Heat Pipe (CLPHP)." Procedia Engineering 105(Icte 2014): 137–44.
- RITTIDECH, S. (2003). "Correlation to Predict Heat Transfer Characteristics of a Closed-End Oscillating Heat Pipe at Normal Operating Condition." Science 23: 497–510.
- WANNAPAKHE, S., T. CHAIWONG, M. DANDEE, and S. PROMPAKDEE. (2012). "Hot Air Dryer with Closed Loop Oscillating Heat Pipe with Check Valves for Reducing Energy in Drying Process." Procedia Engineering 32: 77–82. http://dx.doi.org/10.1016/j.proeng.2012.01.1239.
- XIAN, HAIZHEN *et al.* (2014). "Thermal Characteristics and Flow Patterns of Oscillating Heat Pipe with Pulse Heating." International Journal of Heat and Mass Transfer 79: 332–41. http://dx.doi.org/10.1016/j.ijheatmasstransfer.2014.08.002.
- XIAN, HAIZHEN, YONGPING YANG, DENGYING LIU, and XIAOZE DU. (2010). "Heat Transfer Characteristics of Oscillating Heat Pipe With Water and Ethanol as Working Fluids." Journal of Heat Transfer 132(12): 121501. http://link.aip.org/link/JHTRAO/v132/i12/p121501/s1&Agg=doi (March 2, 2012).
- YANG, HONGHAI, S. KHANDEKAR, and M. GROLL. (2008). "Operational Limit of Closed Loop Pulsating Heat Pipes." Applied Thermal Engineering 28(1): 49–59. http://linkinghub.elsevier.com/retrieve/pii/S1359431107000683 (April 11, 2012).
- YANG, HONGHAI, SAMEER KHANDEKAR, and MANFRED GROLL. (2009). "Performance Characteristics of Pulsating Heat Pipes as Integral Thermal Spread -ers." International Journal of Thermal Sciences 48(4): 815–24.http://dx.doi.org/10.1016/j.ijthermalsci. 2008.05.017.
- YOON, SEOK HUN, and CHEOL OH. (2002). "A Study on the Heat Transfer Characteristics of a Self-Oscillating Heat Pipe." 16(3): 354–62.
- ZHANG, YUWEN, and AMIR FAGHRI. (2002). "Heat Transfer in a Pulsating Heat Pipe with Open End." International Journal of Heat and Mass Transfer 45:755-64.
- ZOHURI, BAHMAN. (2011). Heat Pipe Design and Technology: A Practical Approach. CRC Press.